Are There Real Interdecadal Variations in Marine Low Clouds?

LOUIS J. BAJUK AND CONWAY B. LEOVY

Department of Atmospheric Sciences, University of Washington, Seattle, Washington

(Manuscript received 28 April 1997, in final form 10 November 1997)

ABSTRACT

The dominant interdecadal signal in normalized frequency of occurrence of cumulonimbus reported by volunteer observing ships is globally uniform over the period 1952–92 over all ocean areas between 40°S and 50°N. Globally uniform signals in both normalized frequency of occurrence and amount-when-present also dominate interdecadal variations for other low cloud types. This pattern is inconsistent with plausible physical mechanisms and is apparently due to slow changes in observational practice. Eight ocean weather ships with approximately fixed positions also reported gradual changes in low cloud occurrence frequencies between 1952 and 1969 that were similar in pattern for all eight ships, but for most cloud types these variation patterns differed markedly from those at nearly collocated volunteer observing ships. These apparently spurious variations make it difficult to identify real interdecadal variations in marine clouds from ship observations. However, over the tropical Indian Ocean and central and eastern Pacific Ocean, small but widespread decreases in stratocumulus frequency and increases in deep convective cloud frequency between 1955 and 1978, and 1979 and 1991 tend to be consistently related to changes in sea surface temperature and are likely to be real. Over the western Pacific Ocean, ship reports indicate an increase in the frequency of deep convective clouds between these two periods that is not consistently related to SST changes and is less likely to be real.

1. Introduction

Cloud radiative forcing (CRF) at the top of the atmosphere and at the surface are important components of earth's energy budget that can enhance or diminish climate change through radiative feedback (see reviews by Hartmann 1993 and Wielicki et al. 1995). CRF depends on vertical and horizontal distributions of clouds as well as on cloud solar reflectance and absorptance and cloud infrared emittance. Since CRF changes could be comparable in magnitude to anthropogenic climate forcing factors such as the direct radiative effect of industrially generated aerosols (Slingo 1990; Santer et al. 1995), we were motivated to assess the possibility of using existing cloud data to estimate interdecadal variations in the distribution of marine clouds. The alternative approach of attempting to simulate retrospective cloud changes using atmospheric general circulation models is suspect at this time because of unresolved errors in model cloud distributions (Barker et al. 1994; Haskins et al. 1995; Cess et al. 1996).

Satellite datasets, such as those produced by the International Satellite Cloud Climatology Project (ISCCP; Rossow and Schiffer 1991), are potentially useful for study of interdecadal cloud variations, but these records are short (the ISCCP record begins in July 1983) and continuing effort is required to remove effects of changing instrument calibrations on cloud retrievals (e.g., Klein and Hartmann 1993; Brest et al. 1996).

Surface observations are also available. Interannual and interdecadal variations of cloud cover derived from surface observations have previously been reported over land (e.g., Henderson-Sellers 1992) and over oceans (Warren et al. 1988; London et al. 1991; Bajuk and Leovy 1998). Warren et al. (1988) have compiled atlases of cloud coverage by cloud type from the archives of the Comprehensive Ocean Atmosphere Data Set (COADS). London et al. (1991) pointed out that these data show an apparent increase in sky coverage by tropical marine cumulonimbus clouds (Cb) over the 29-yr period 1952–81 amounting to almost 50%. They suggested that part of the apparent tropical Cb coverage trend could be due to changes in coding instructions or subjective differences between observers, but their results were reported as a possible long-term change in the 1995 review by the Intergovernmental Panel on Climate Change (see Nicholls et al. 1996, 162–163). The purpose of this paper is to reexamine and extend the analysis of the COADS cloud observations using the screening procedures developed by Hahn et al. (1994) in order to better assess the reliability of the apparent Cb trend as well as any other interdecadal variations in marine convective or stratiform clouds.

Corresponding author address: Conway B. Leovy, University of Washington, Department of Atmospheric Sciences, Box 351640, Seattle, WA 98195-1640.
E-mail: conway@atmos.washington.edu

TABLE 1. Ocean weather ships used in this study.

Ship	Nominal location	Operating countries
C	52°45′N, 35°30′W	United States/Soviet Union
D	44°00′N, 41°00′W	United States
E	35°00′N, 48°00′W	United States
J	52°30′N, 20°00′W	United Kingdom/the Netherlands
K	45°00′N, 16°00′W	Belgium/France/the Netherlands
N	30°00′N, 140°00′W	United States
P	50°00′N, 145°00′W	Canada
V	34°00′N, 154°00′E	United States

2. Data and analysis

a. Cloud observations

The cloud observations used in this study were obtained from the collection of individual surface observations in COADS archives (Woodruff et al. 1987) and processed using algorithms similar to those used for the Edited Cloud Report Archive (ECRA) dataset (Hahn et al. 1994) by J. Norris (Norris 1998b). Most of the observations are from volunteer observing ships (VOS) spanning December 1951–December 1992, but observations from some ocean weather ships (OWS) at approximately fixed positions are also used.

Surface observers normally report total cloud cover, lower cloud amount, and low, middle, and high cloud types, if visible to the observer. These reports are used to calculate the average frequency of occurrence of each cloud type (FQ) and the average low cloud sky coverage when that cloud was present (amount-when-present, or AWP). Average cloud amount (AMT) is the product of these two values (AMT = FQ × AWP). Cloud type identification is made according to a system of classification from the World Meteorological Organization code (WMO 1956, 1975; see Bajuk and Leovy 1998, Table 1). Only one low cloud type can be reported in an observation. The choice of which low cloud type to report, if multiple types are present, is made according to a strict hierarchy. If any cumulonimbus (Cb) with anvil (CL9), Cb without anvil (CL3), stratocumulus (Sc) formed from the spreading of cumulus (CL4), cumulus (Cu) and stratocumulus mixed at different levels (CL8), or large cumulus (CL2) is present, it is reported as the low cloud type in that order of preference. Otherwise, the low cloud type is reported as whichever of the following covers the largest area of sky: small Cu (CL1), Sc not formed from Cu (CL5), stratus (St) other than stratus of bad weather (CL6), or ragged stratus or cumulus of bad weather (CL7).

Biases and spurious trends in FQ or AWP can arise from systematic changes in procedures given to observers, changes in the interpretation of these procedures, changes in the mix of ships with different observing conditions, and changes in ship routing or times of observations. For example, systematic tendencies for certain groups of ships to avoid bad weather or systematic changes in the ratio of daylight to total observations could introduce a spurious trend in observed cloud amount. A well-documented change in cloud identification codes occurred in the late 1940s. The previous cloud code (Berry et al. 1945) did not define the cloud groups as uniquely as the modern code. Large shifts in FQ of several cloud types in the cloud record in the early 1950s (see Fig. 4) are likely to be the result of the new cloud code slowly percolating through the VOS system.

b. Sea surface temperatures and surface wind divergence

Because the distributions of marine boundary layer cloud types are intimately related to boundary layer processes and sea surface temperature (Norris 1998a; Bajuk and Leovy 1998), we have also carried out a limited examination of relationships between cloud changes by type and changes in sea surface temperature (SST) and surface wind divergence. Sea surface temperature was obtained from the *Global Ocean Surface Temperature Atlas* (*GOSTA*) dataset (Bottomley et al. 1990) and averaged onto a 10° × 20° grid of monthly means for comparison with the cloud observations. Surface wind divergence was obtained from COADS winds aggregated to a 5° × 5° grid for the time periods of interest, with divergence further averaged to the 10° × 20° grid. We did not attempt to correct divergence for possible systematic changes in wind speed errors (Wright 1986).

c. Analysis

Data were averaged into monthly means of FQ and AWP on a modified 10° latitude by 20° longitude grid, as in Bajuk and Leovy (1998). These have been further averaged into annual average time series, and a 3-yr running mean has been applied, yielding a smoothed 39-yr dataset (1953–91) in each 10° × 20° grid box. To examine the behavior of Cb more closely, the observations for low cloud types CL3, CL9 (Cb without and with anvil, respectively), and CL10 were added to create a total Cb field. CL10 is the designation used for a report of a thunderstorm (current weather codes 80–99) with sky obscured (Warren et al. 1988). Because observations of Cb are sparse north of 50°N, and all ship observations are sparse south of 40°S, we present results only for the region between 40°S and 50°N.

Almost all of the available cloud observations were obtained from VOS. To assess possible systematic differences in FQ obtained by observers with different backgrounds of training and experience, we compared observations made at eight OWS operated by several different meteorological services with nearby VOS observations. OWS monthly cloud type data from December 1951 to December 1969 were used to create annual averages from 1952 to 1969. A 3-yr running mean was applied yielding 16 yr of smoothed data (1953–68). OWS and VOS data were averaged over 5° × 5° grid

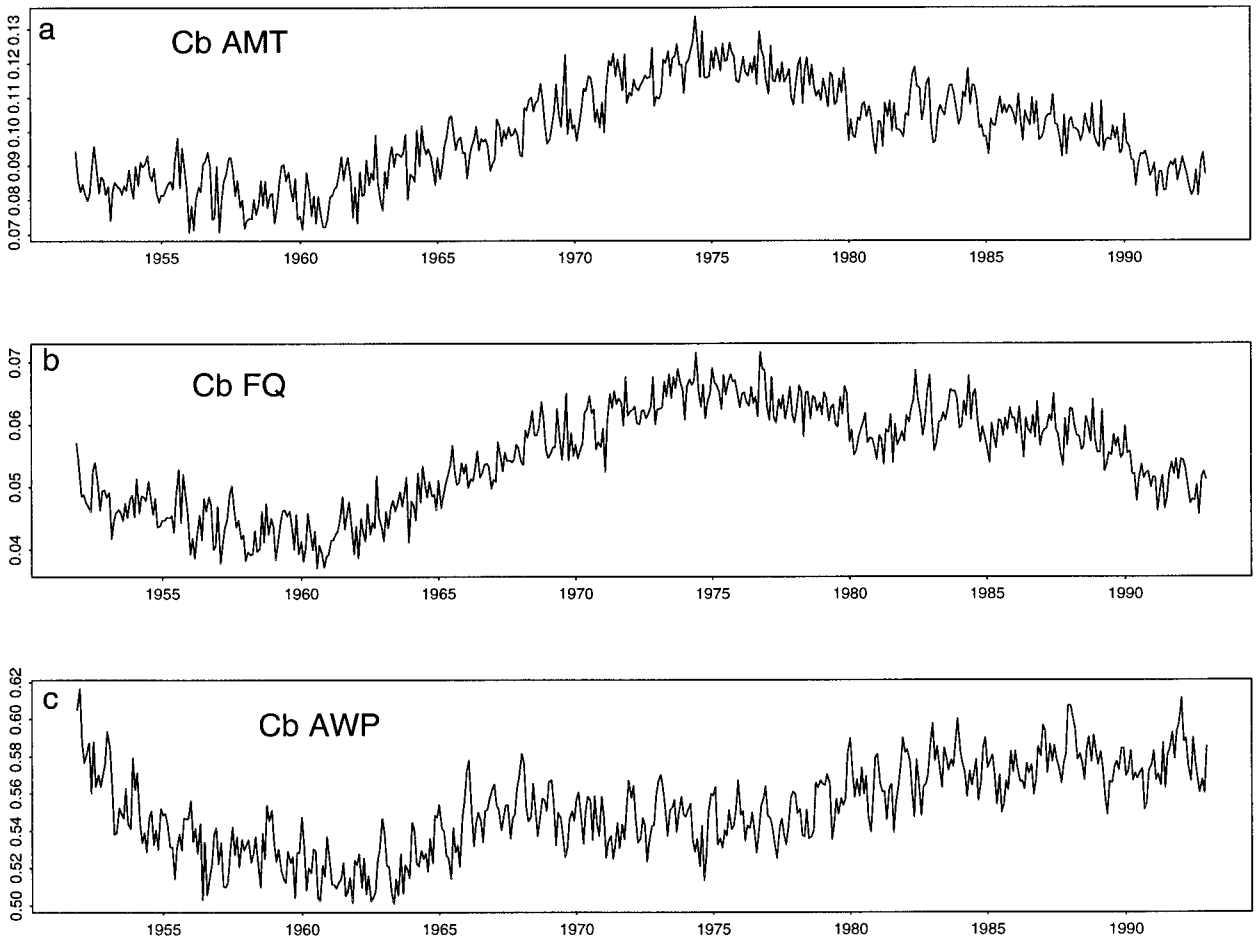

FIG. 1. Total cumulonimbus (a) AMT, (b) FQ, and (c) AWP monthly and globally averaged for December 1951–December 1992. Total Cb is the sum of Cb with and without anvil and reports of thunderstorm with sky obscured (CL3 + CL9 + CL10).

boxes centered on eight nominal OWS locations in the North Atlantic and North Pacific Oceans (Table 1). At each location, the FQ of each cloud type was calculated separately for OWS and VOS observations.

3. Observed interannual variations of cumulonimbus

Because of the large size of the relative change in Cb reported by London et al. (1991) and the potential significance of Cb as a measure of the frequency of deep convection (Soden and Fu 1995), we first performed an analysis of the Cb variations to determine the relative contributions of FQ and AWP to AMT and to investigate the global pattern of the low-frequency variations.

Figure 1 shows monthly time series for Cb AMT, FQ, and AWP, averaged over the entire globe after binning into grid boxes. The Cb amount increased steadily from 1960 to around 1975, then decreased from 1975 to 1992. It is evident that the change in average AMT is due to a change in the FQ of Cb, rather than AWP. Linear correlation of Cb FQ with AMT explains 92% of the variance of AMT, but only 18% of AMT variance is explained by linear correlation with AWP.

Figure 2a illustrates the global character of these trends in Cb FQ by displaying averages over 10° latitude bands from 40°S to 50°N. The global average of all grid boxes (the annually averaged version of Fig. 1b) is also superimposed. Tropical latitudes, which have the highest climatological Cb amount, also have the largest trends. An even clearer pattern emerges when the time series for each latitude band is normalized by dividing each time series including the global annual average (heavy solid line in Fig. 2b) by its climatological mean. Low-frequency variations in normalized Cb FQ have been essentially the same in each latitude band despite variations by nearly a factor of 3 between the means for the different latitude bands (Fig. 2a, Table 2). The Cb FQ increased from about 80% of its long-term zonal mean in 1960 to about 120% of its mean in 1975, and then decreased again to slightly below its climatological mean value by 1992. Poleward of the 40°S–50°N latitude band, the general behavior is similar though less clear due to noise from sparse data sampling.

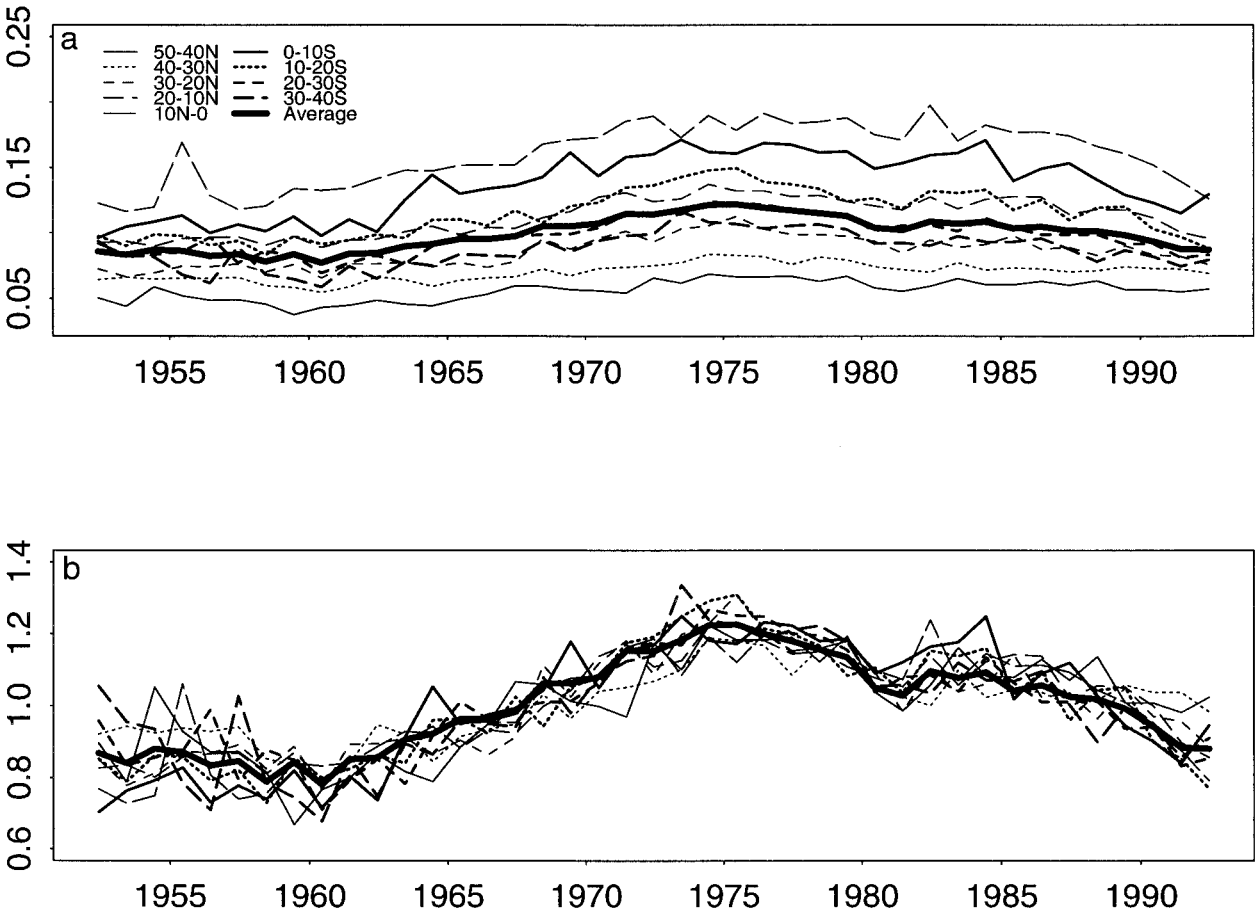

FIG. 2. Total Cb FQ, annually averaged and smoothed with a 3-yr running mean. (a) Zonally averaged for each 10° latitude band for 50°N–40°S. The global annual average Cb FQ (heavy line) is included for comparison. (b) Same as (a) but normalized by dividing by the 39-yr mean in each latitude band. The global annual average, divided by its long-term mean, is plotted as the heavy line.

TABLE 2. Values of FQ (upper rows) and AWP (lower rows) of low cloud types averaged over latitude bands.

Cloud type	1 Small Cu	2 Large Cu	3 Cb w/o anvil	4 Mixed Cu and Sc	5 Sc	6 Stratus	7 Bad weather Cu Sc	8 Cu and Sc at diff levels	9 Cb with anvil
50°–40°N	0.08	0.08	0.04	0.18	0.12	0.12	0.10	0.09	0.02
	0.37	0.51	0.59	0.65	0.82	0.89	0.87	0.77	0.70
40°–30°N	0.15	0.15	0.06	0.09	0.14	0.07	0.08	0.09	0.02
	0.33	0.46	0.54	0.60	0.76	0.82	0.82	0.72	0.65
30°–20°N	0.21	0.21	0.08	0.08	0.09	0.03	0.04	0.08	0.02
	0.30	0.41	0.48	0.55	0.70	0.75	0.77	0.66	0.57
20°–10°N	0.22	0.23	0.09	0.07	0.06	0.03	0.04	0.06	0.02
	0.30	0.40	0.47	0.52	0.66	0.70	0.73	0.63	0.55
10°N–0°	0.20	0.25	0.12	0.07	0.07	0.03	0.06	0.08	0.04
	0.31	0.41	0.50	0.54	0.70	0.77	0.77	0.67	0.60
0°–10°S	0.24	0.26	0.10	0.06	0.08	0.02	0.04	0.06	0.04
	0.29	0.39	0.48	0.51	0.69	0.75	0.76	0.65	0.56
10°–20°S	0.22	0.23	0.09	0.07	0.12	0.03	0.05	0.07	0.03
	0.30	0.41	0.49	0.54	0.72	0.77	0.76	0.67	0.58
20°–30°S	0.20	0.20	0.07	0.08	0.14	0.04	0.06	0.08	0.02
	0.29	0.41	0.50	0.54	0.73	0.79	0.79	0.68	0.58
30°–40°S	0.15	0.14	0.06	0.08	0.19	0.06	0.08	0.08	0.02
	0.30	0.43	0.53	0.55	0.75	0.82	0.82	0.69	0.62

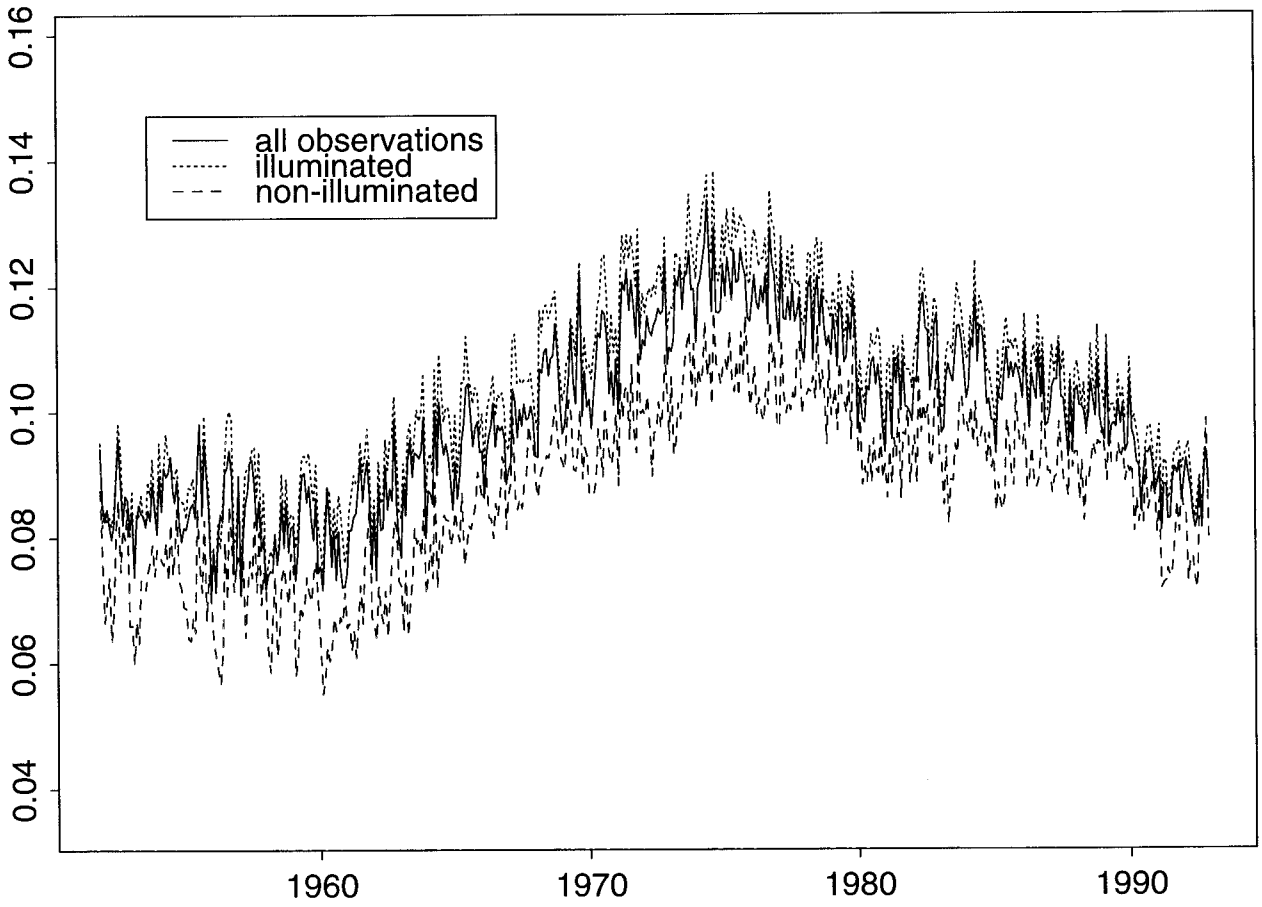

FIG. 3. Global average Cb FQ for illuminated and nonilluminated conditions, using the illumination criterion of Hahn et al. (1995), as well as for all observations.

Empirical orthogonal function analysis on the monthly Cb FQ data (not shown) yielded similar results. The long-term variation in Cb FQ corresponds to the first principle component of nonseasonal Cb FQ, and the corresponding physical pattern is uniform in sign throughout the globe. Variations of CL3 and CL9 both contribute to this pattern, though with different contributions at different times. The contribution of CL10 is always very small.

The global nature of this pattern is inconsistent with a physical mechanism. For example, Bajuk and Leovy (1998) showed a consistent relationship between Cb frequency and SST in the Tropics on seasonal and interannual timescales that plausibly reflects control of Cb frequency by static stability. But the low-frequency SST variations during the period of greatest apparent change in Cb FQ, 1960–75, vary widely across the various latitude bands of Fig. 2a and are generally negative in the Northern Hemisphere and positive in the Southern Hemisphere (Oort et al. 1987), so that interdecadal correlations between Cb frequency and SST are of opposite sign in the two hemispheres. While interannual variations of Cb are inconsistent with a physical mechanism related to SST variations, they are consistent with slow globally diffused changes in VOS practices for observing and reporting Cb, or with globally systematic changes in observing conditions.

The Cb FQ may be particularly sensitive to observer bias since it must be reported even if a single Cb is visible in a field of other low clouds. Observations of Cb could be particularly sensitive to illumination conditions so that changes in the distribution of ships relative to illumination or local time could introduce spurious long-term variations. To investigate this possibility, we segregated the data by day and night, by illuminance conditions at the time of observation (see Hahn et al. 1995), and by local time. The results (Fig. 3) indicate that, while there is a systematic illumination dependence in reported Cb FQ, very similar long-term variation is present in both day and night observations as well as in data screened to accept only observations under relatively good illumination.

Changes in shipping routes or mix of observing ship types can create a spurious change in observed variables (Quayle 1974; Wright 1986; Warren et al. 1988). Average ship size in the world merchant fleet increased

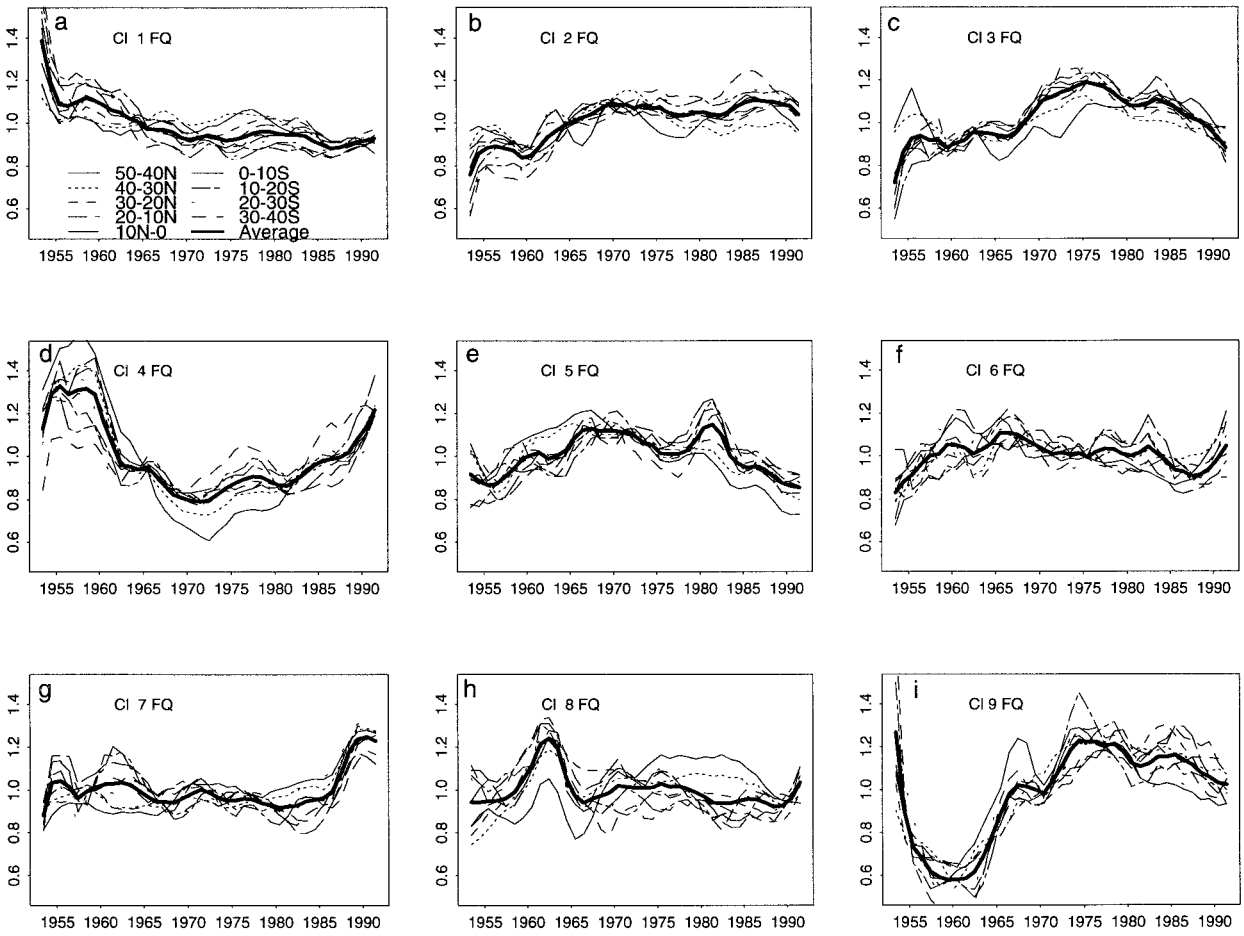

FIG. 4. Normalized annually averaged frequencies for low cloud types CL1–CL9 with 3-yr running mean applied by 10° latitude band 40°N–50°S, for 1952–92. Each line represents the average for a particular cloud type and latitude band. The heavy line in each plot represents the average over the nine latitude bands. All frequencies are normalized by the 39-yr mean for that latitude band.

approximately 50% between 1960 and 1990, driven largely by an increase in the number of large tankers (Stopford 1988; Gardiner 1992). Viewing conditions and use of weather information for route selection may be different for these large ships than for smaller vessels. Between 1960 and the early 1980s, the growth in the tanker fraction of the merchant fleet paralleled the global growth in FQ of Cb, but oil tankers tend to concentrate on specific routes, so this factor alone is unlikely to account for the apparent globally uniform trends.

We reviewed the instructions given to observers (WMO 1956, 1975) but could find no systematic change in observing procedures that could explain spurious Cb trends. However, if systematic changes in practices are responsible, we expect to find related variations in other cloud types. If Cb FQ increased from 1960 to 1975 because observers were more likely to call a particular cloud cumulonimbus (e.g., as opposed to cumulus or cumulus growing into stratocumulus), then there should be compensating decreases in the frequencies of other cloud types. In the next section, we examine variations of FQ and AWP for all stratiform and convective (low) cloud types.

4. Interannual variations of FQ and AWP for all low cloud types

a. Behavior of the individual cloud types

In Figs. 4 and 5, smoothed annual mean FQ and AWP of each of the nine cloud types of Table 1 are shown segregated by latitude band. In order to clearly display the similarities between observations in different latitude bands, all FQs have been normalized as in Fig. 2b, and the climatological means of AWP in each latitude band have been subtracted from the annual means in that band. The corresponding area averages for the region 40°S–50°N are also shown as heavy lines. Table 2 contains the average FQ and AWP at each latitude for each cloud type and can be used to scale the time series in Figs. 3 and 4 to each latitude band.

It is evident from Fig. 3 that FQ and AWP of each

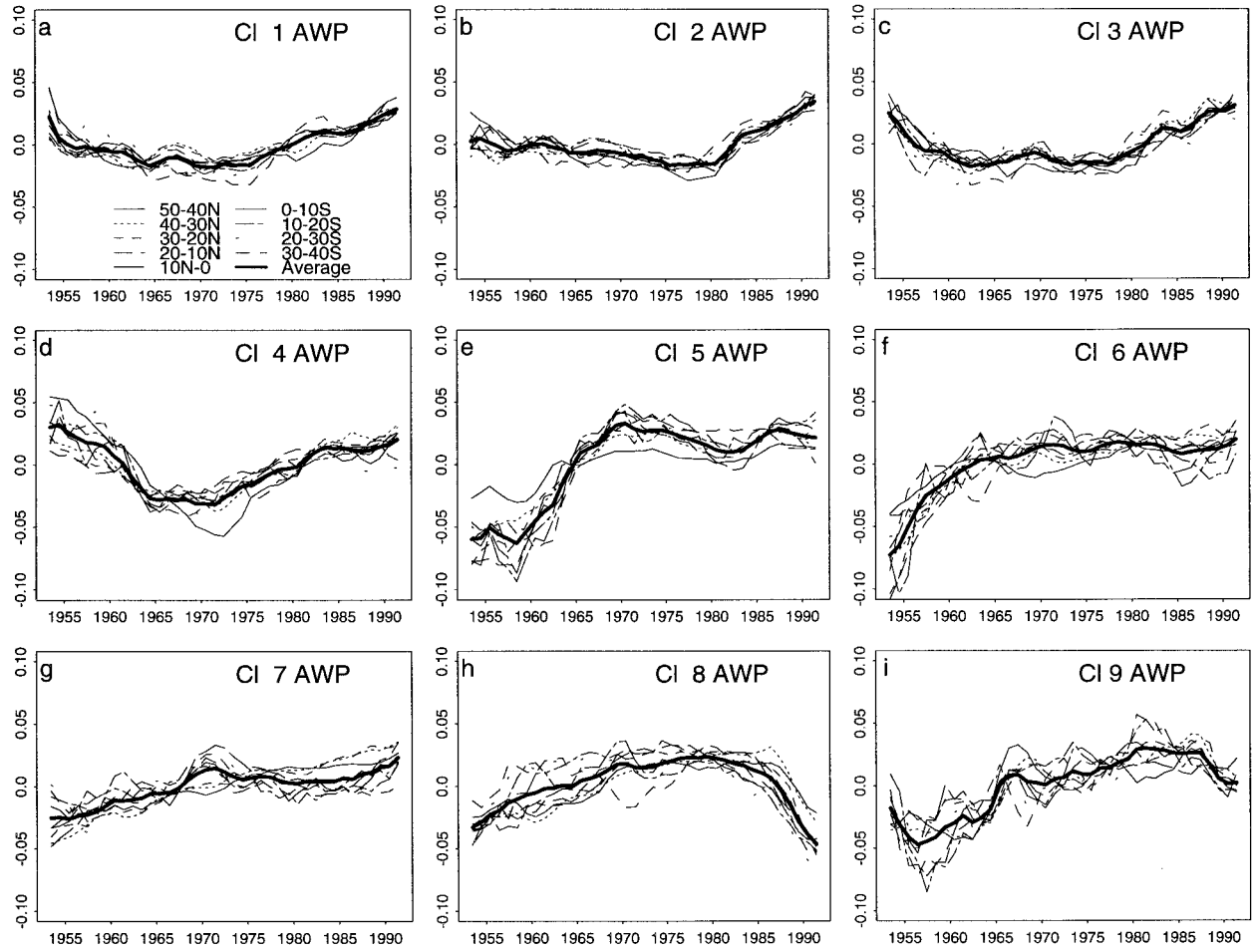

FIG. 5. As in Fig. 3 but for average AWP for the nine cloud types in 10° latitude bands. Instead of normalizing AWP, the mean of each time series has been subtracted.

low cloud type varies in a similar way across all latitude bands between 40°S and 50°N. Since all low cloud types are included in our analysis, an increase in FQ of a given cloud type due to a change in cloud identification should be reflected in a decrease in the FQ of other cloud types. By far the most striking trade-off between two cloud types is between small and large Cu (CL1 and CL2). The correlation between the time series of these two cloud types is −0.96 (Fig. 6). Especially early in the period, the average boundary between small and large cumulus specified by observers was shifting. Anticorrelation between FQ of stratocumulus formed by spreading out of cumulus (CL4) and plain stratocumulus (CL5) suggests that observer identification trade-offs between these two cloud types has been important (Fig. 6), but identifications of Cb (CL3 and CL9) and mixed stratocumulus and cumulus (CL8) also appear to be involved in these trade-offs. The data do not suggest any clear-cut trade-offs between Cb types and any other single low cloud type. Near-global averages of the summed frequencies of the pure stratiform cloud types CL6–CL8 exhibit little long-term variability, except for a small spike in the early 1960s due to a spike in CL8 (cumulus and stratocumulus at different levels) and a gradual increase in CL7 (ragged stratus or cumulus of bad weather) beginning in the 1980s.

In order to further explore the spatial patterns of these variations, correlation-based EOF analysis was performed on the gridded cloud data. For most cloud types, a global mode of uniform sign constitutes the dominant mode of long-term variability in FQ and AWP. Variations in FQ of CL1–CL5 and CL9 are dominated by a single mode, positive over most of the world's oceans, that explains over 30% of the variance in each case. The FQ of CL7 also shows such a mode, with 26% of the variance explained. Furthermore, the time series associated with these modes resemble the simple global averages from Fig. 4, with correlations of 0.9 or greater. The FQ of CL 6 (stratus) and CL 8 (cumulus and stratocumulus at different levels) show a different behavior with a leading mode that is less globally uniform and with a lower correlation with the curves shown in Fig. 4. EOF analysis was also performed on AWP for each cloud type. All cloud types except CL7 are dominated

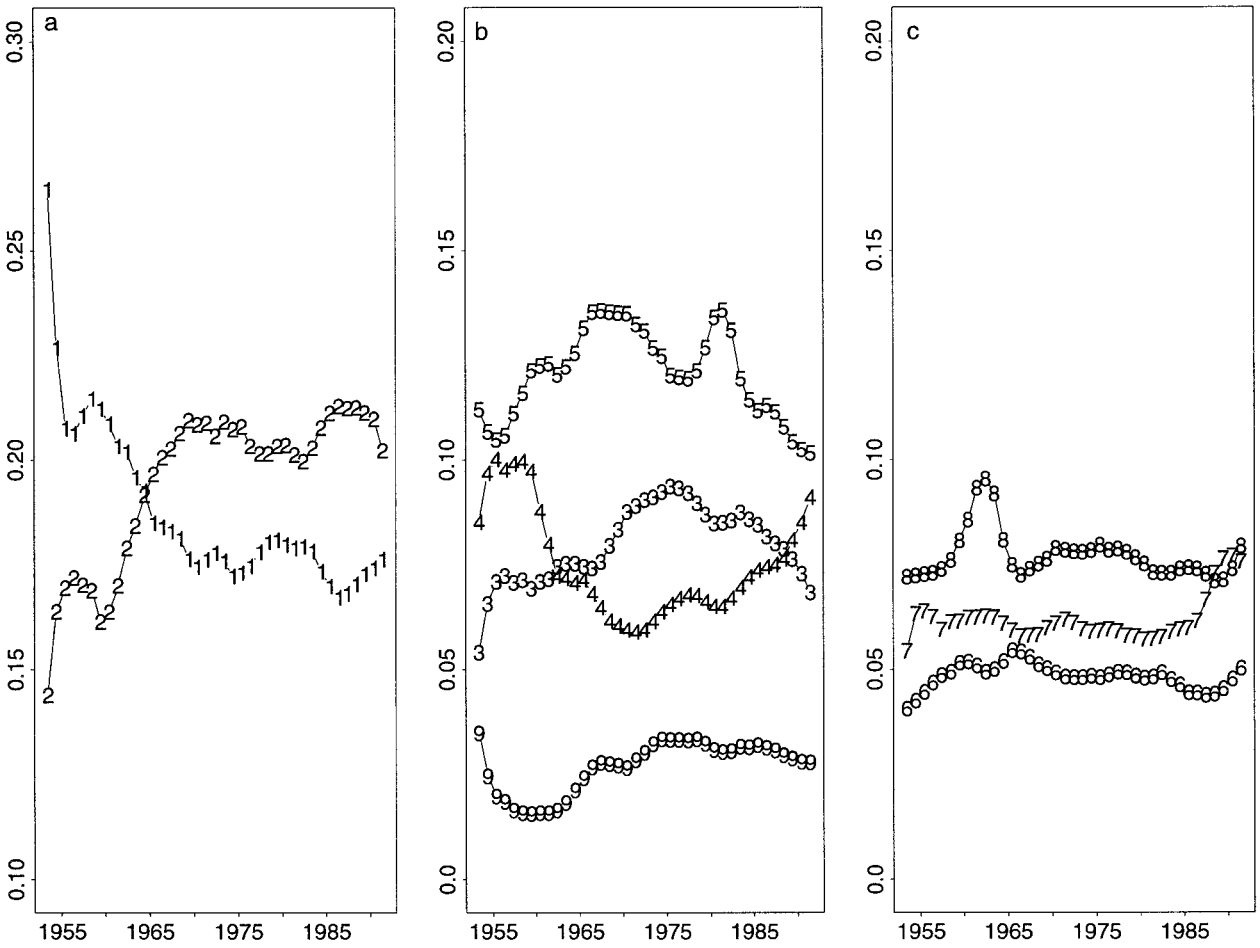

FIG. 6. Near-global (40°S–50°N) averages for (a) CL1 and CL2; (b) CL3, CL4, CL5, CL9; and (c) CL6–CL8. All three plots have the same scale but different origins.

by a globally consistent mode of variation of AWP that explains 30%–50% of the variance and is generally well correlated with the global mean variation for each cloud type.

b. OWS–VOS comparisons

Analysis of the OWS data revealed that long-term variability of normalized FQ was significant but very similar for each OWS despite their widely different locations. Since the OWS are located in a wide range of marine climatic regimes, this suggests a dominant component of interannual variation associated with slowly changing practices of the OWS observers but unrelated to real climate changes. Variations of the VOS in 5° × 5° boxes near each OWS and averaged over all eight OWS locations tended to follow the global pattern of the VOS variation of FQ, especially for the more common cloud types. However, that pattern is different from that of the OWS for most cloud types. Correlations between the global average time series and the time series for the OWS and nearby VOS are given in Table 3. Note the negative values for CL2 and CL5–CL9. Changing observing practices seemed to be affecting FQ observed at all OWS in much the same way but differently from the mean FQ observed at VOS. This makes it very difficult to use the OWS time series as a basis for a correction to the VOS observations, even for the period when the OWS data were available.

c. Relationships between cloud FQ changes and changes in SST

For both seasonal mean climatologies and variations associated with El Niño–Southern Oscillation (ENSO), Bajuk and Leovy (1998) found consistent relationships between FQ of lower cloud types and SST and/or surface wind divergence over much of the tropical Indian and Pacific Oceans. This was illustrated by plotting ''standard anomalies'' of FQ of selected lower cloud types against SST or divergence as arrows. Each standard anomaly arrow represented the change in FQ for a change in SST or divergence in a 10° lat × 20° long grid box corresponding to one standard deviation of an

TABLE 3. Correlation coefficient between global average time series (Fig. 3) and VOS and OWS in collocated 5° × 5° grid box.

Cloud type	1 Small Cu	2 Large Cu	3 Cb w/o anvil	4 Mixed Cu and Sc	5 Sc	6 Stratus	7 Bad weather Cu/Sc	8 Cu and Sc at diff levels	9 Cb with anvil
VOS	0.88	0.91	−0.55	0.94	0.97	0.61	0.83	0.64	0.89
OWS	0.67	−0.37	0.52	0.71	−0.93	−0.76	−0.39	−0.11	0.39

ENSO index obtained from linear regression analysis. Consistent relationships were demonstrated by parallelism between the standard anomaly vectors and curves representing the multiyear average relationships. Consistency between anomalies and multiyear averages was taken to indicate a consistent physical mechanism linking SST or surface wind divergence with FQ.

We applied this methodology to the interdecadal variations investigated here. First, change relationships between the time periods 1957–61 and 1973–77 in FQ and SST for five cloud type groups (CL5, CL4 + CL8, CL1, CL2, CL3 + CL9 + CL7) were investigated. These time intervals were chosen to correspond to the largest globally uniform changes in normalized cloud FQ when spurious change is expected to be large. The cloud type groups were chosen to correspond to stratified boundary layers, transitional boundary layers, and three convective boundary layer classes ranging from shallow to deep. Analysis was limited to the Indian and Pacific Oceans between 30°S and 30°N. As expected for a spurious effect, changes in FQ were generally much larger than the change expected for the observed SST change, were nearly uniform in magnitude and direction over the whole region despite differences in SST variations over the region, and were nearly orthogonal to the direction of climatological variations in the FQ–SST plane (Fig. 7). Stratocumulus (CL5) was an exception, showing smaller changes and more of a tendency for the arrows to parallel climatology.

The same analysis method does suggest real FQ

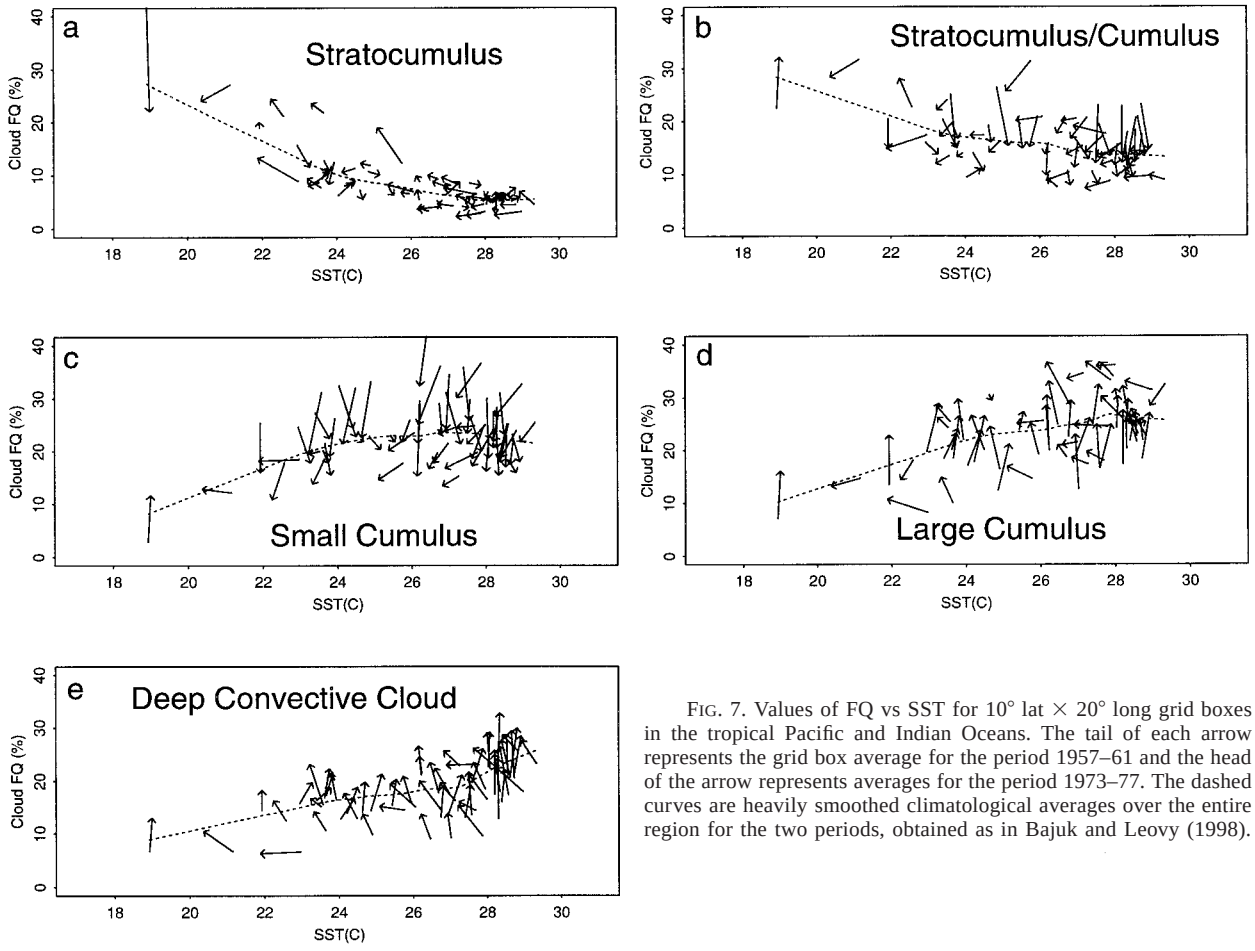

FIG. 7. Values of FQ vs SST for 10° lat × 20° long grid boxes in the tropical Pacific and Indian Oceans. The tail of each arrow represents the grid box average for the period 1957–61 and the head of the arrow represents averages for the period 1973–77. The dashed curves are heavily smoothed climatological averages over the entire region for the two periods, obtained as in Bajuk and Leovy (1998).

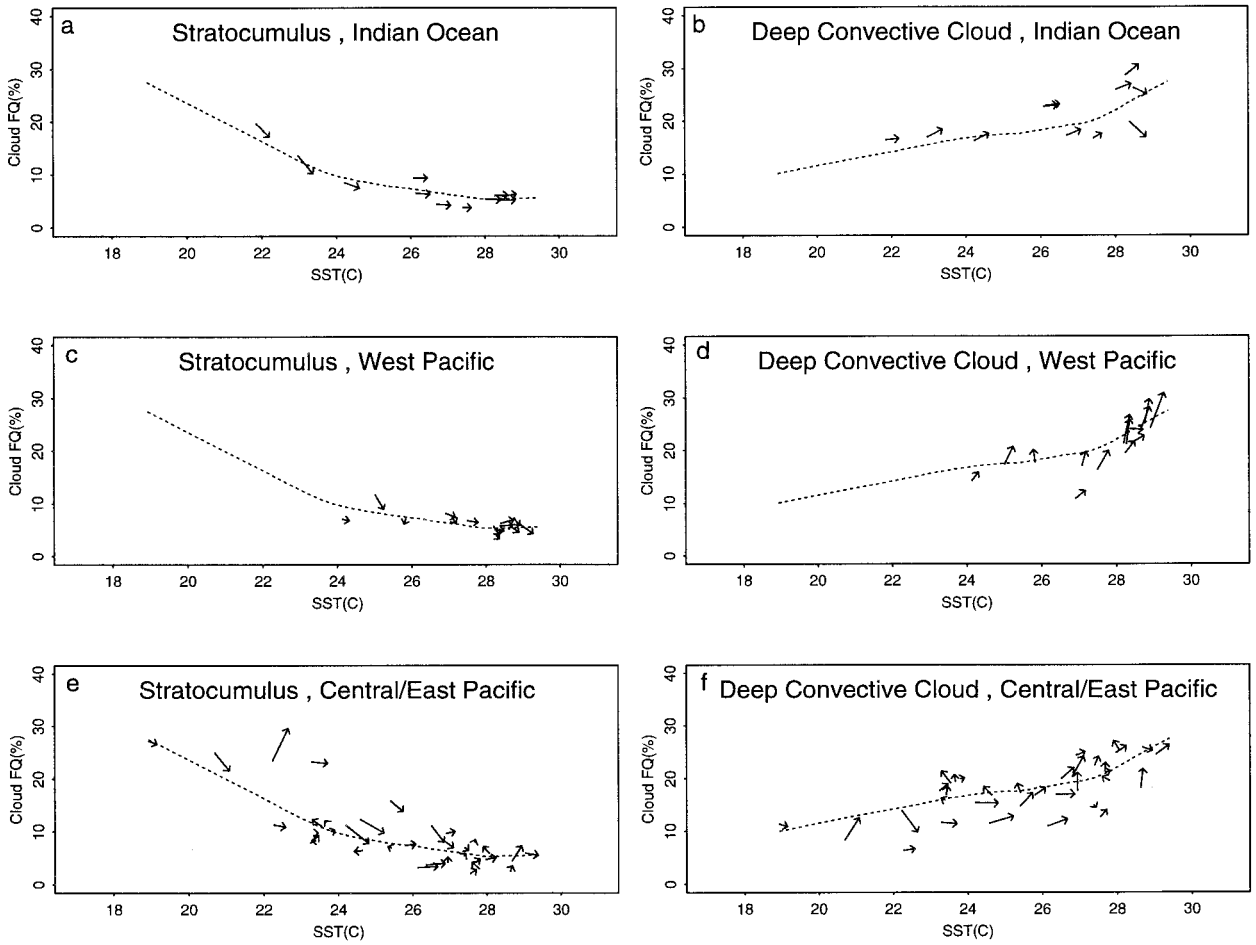

FIG. 8. Same as Fig. 5 for changes in grid box averages from 1955–78 (arrow tails) to 1979–91 (arrowheads) for stratocumulus (left panels) and deep convective clouds (right panels) for three regions: (a) and (b) west of 100°W, (c) and (d) 100°–140°E, and (e) and (f) east of 160°E.

changes in the tropical Pacific and Indian Oceans between 1955–78 and 1979–91. Previous studies (Nitta and Yamada 1989; Mitchell and Wallace 1996) have reported changes in tropical background SST and other variables during the late 1970s. East tropical Pacific SST has been almost 0.5°C warmer in the 1980s and 1990s than in the 1960s and 1970s. While changes in cumulus and mixed stratocumulus types (CL1, CL2, and CL4 + CL8) again seemed dominated by observational artifacts (not shown), much of the change in stratocumulus (CL5) and deep convective clouds (CL3 + CL9 + CL7) was systematically related to SST and may be real. Figure 8 shows FQ versus SST for these cloud type groups for three tropical ocean regions: the Indian Ocean, the western Pacific, and the eastern and central Pacific. In the eastern and central Pacific and in the Indian Ocean regions, there is a marked tendency for arrow slopes to follow the multiyear mean for both stratocumulus and deep convective clouds, although there is considerable scatter for the latter group. An arbitrary measure of this tendency is the occurrence frequency of arrow directions within 30° of the slope of the multiyear FQ–SST curve at the same SST value (Table 4). The high values of this occurrence frequency for all Table 4 entries except Cb cloud types over the western Pacific are consistent with, but do not prove, a physical connection between FQ and SST changes between these periods. Spatial aspects of these variations are displayed in Fig. 9.

TABLE 4. Frequencies of occurrence of directions of standard anomaly arrows in Fig. 8 within 30° of the climatological slope of FQ versus SST at the same SST value. (Expected frequency for random direction = 0.17.) Values in parentheses correspond to east–central Pacific cases in which the change in SST over the period exceeded 0.2°C. Twenty-one out of 34 bins are included in this group.

	CL5	Cb + CL7
Indian Ocean	1.00	0.73
West Pacific	0.57	0.29
East–central Pacific	0.41 (0.62)	0.41 (0.57)

The most significant feature in the spatial pattern of change of surface wind divergence (not shown) is a weak convergence increase centered near 5°S in the cen-

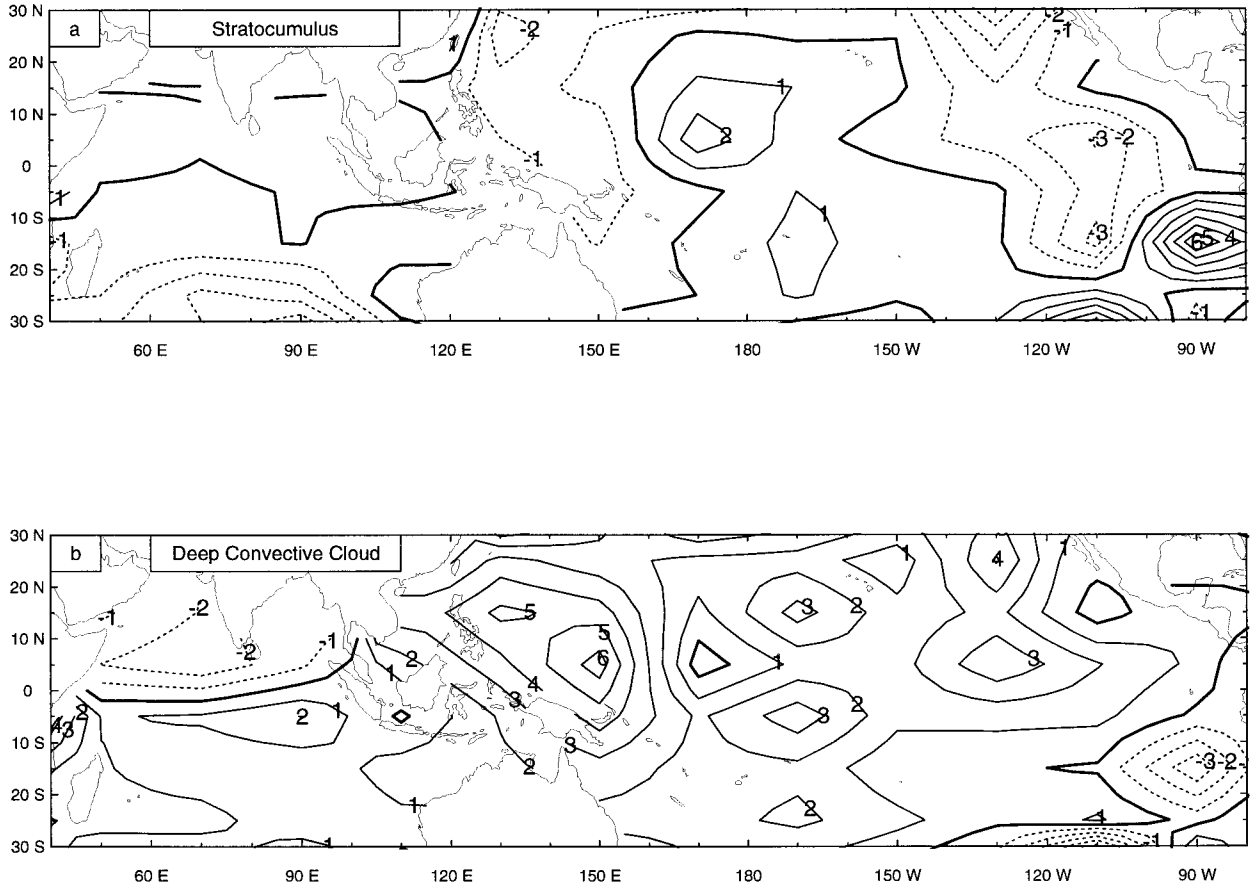

FIG. 9. Spatial distribution of changes between the periods 1955–78 and 1979–91 in the tropical Pacific and Indian Oceans corresponding to the arrows plotted in Fig. 8 for (a) stratocumulus, (b) deep convective cloud, and (c) SST.

tral Pacific, where small increases in Cb FQ also occurred. In the region of largest apparent change in Cb FQ (10°S–20°N, 120°–150°E) where changes reach or exceed 4% (Fig. 9), divergence change is varied, becoming more convergent in the northern portion and more divergent in the southern portion between the two periods. Systematic indications of change in circulation or convective activity have been reported in this region in other studies. Mitchell and Wallace (1996) showed an increase (decrease) in the strength of the trade winds during the warm season (January–May) during the positive (negative) phase of ENSO. This change may be related to the annual mean divergence change noted above.

Graham (1994) has analyzed a coupled mode of variation of SST and highly reflective cloud (HRC) that exhibits an increase in HRC during boreal winter between 1970–71 and 1985–86 within and to the southeast of this 10°S–20°N, 120°–150°E region. However, linear trends in outgoing longwave radiation (OLR) and HRC between the early 1970s and late 1980s support a pattern of convective cloudiness change that is quite different from that shown in Fig. 9b (Waliser and Zhou 1997). After removal of biases due to satellite orbit changes, OLR shows small decreases, expected to correspond to small increases in deep convective cloud, and HRC shows mixed changes in the 10°S–20°N, 120°–150°E region, but both OLR and HRC indicate large changes in convective cloudiness farther east, centered near 5°S, 175°W. If the OLR changes reported by Waliser and Zhou are convolved with the linear relationship between OLR and deep convective cloud found by Bajuk and Leovy (1998), a deep convective cloud increase of slightly less than 2% would be inferred for the region 10°S–20°N, 120°–150°E, and an increase of about 4% would be inferred for the region near 5°S, 175°W.

5. Conclusions

Three pieces of evidence strongly indicate that the interdecadal variations in the ship record of low cloud FQ are dominated by observational artifacts: 1) the globally uniform spatial structure of normalized means, 2) differences between the patterns of variation at OWS and nearby VOS, and 3) generally inconsistent relationships between variations of cloud FQ and SST and cloud FQ and divergence. AWP of low cloud types also show subtle globally systematic interdecadal changes

that are likely to be artifacts. However, small decreases in FQ of stratocumulus (CL5) and small increases in FQ of deep convective clouds (Cb + CL7) that are generally consistent with SST changes occurred over the tropical Pacific and Indian Oceans between 1955–78 and 1979–91, intervals over which significant changes in a number of climate variables have been previously reported. Much of the FQ change in these cloud types between these two periods may be real and associated with corresponding changes in the intensity and structure of ENSO events (Mitchell and Wallace 1997).

Acknowledgments. We thank Joel Norris, Steve Warren, and Carole Hahn for preparation of the screened cloud dataset from the COADS observations and for making these observations available to us. We also thank Joel Norris and Stephen Warren for helpful comments on an earlier version of this manuscript. The U.K. Meteorological Office kindly provided the *GOSTA* dataset. This work was supported by an Earth Observing System Grant (NASA NAGW-2633).

REFERENCES

Bajuk, L., and C. Leovy, 1998: Seasonal and interannual variations in stratiform and convective clouds over the tropical Pacific and Indian Oceans from ship observations. *J. Climate,* **11,** 2922–2941.

Barker, H. W., Z. Li, and J.-P. Blanchet, 1994: Radiative characteristics of the Canadian Climate Centre second-generation general circulation model. *J. Climate,* **7,** 1070–1091.

Berry, F. A., E. Bollay, and N. R. Beers, 1945: *Handbook of Meteorology.* McGraw-Hill, 1068 pp.

Bottomley, M., C. K. Folland, J. Hsiung, R. E. Newell, and D. E. Parker, 1990: *Global Ocean Surface Temperature Atlas.* U.K. Meteorological Office and Massachusetts Institute of Technology, Department of Earth, Atmopheric, and Planetary Sciences, 20 pp. and 313 maps. [Available from Dept. of Earth, Atmospheric and Planetary Sciences, MIT, Cambridge, MA 02139.]

Brest, C. L., W. B. Rossow, and M. D. Roiter, 1996: Update of radiance calibrations for ISCCP. *J. Atmos. Oceanic. Technol.,* **14,** 1091–1109.

Cess, R. D., and Coauthors, 1996: Cloud feedback in atmospheric general circulation models: An update. *J. Geophys. Res.,* **101,** 12 791–12 794.

Gardiner, R., 1992: *The Shipping Revolution: The Modern Merchant Ship.* Naval Institute Press, 208 pp.

Graham, N. E., 1994: Decade scale climate variability in the tropical and North Pacific during the 1970s and 1980s: Observations and model results. *Climate Dyn.,* **10,** 135–162.

Hahn, C. J., 1995: The effect of moonlight on cloud cover observations at night, and application to cloud climatology. *J. Climate,* **8,** 1429–1446.

——, S. G. Warren, and J. London, 1994: Edited synoptic cloud reports from ships and land stations over the globe, 1982–1991. Carbon Dioxide Information Analysis Center Tech. Rep., Oak Ridge National Laboratory, Oak Ridge, TN, 45 pp. [NTIS NDP0268.]

Hartmann, D. L., 1993: Radiative effects of clouds on Earth's climate. *Aerosol–Cloud–Climate Interactions,* Academic Press, 151–173.

Haskins, R. D., T. Barnett, and M. Tyree, 1995: Comparison of cloud fields from atmospheric general circulation model, in situ and satellite measurements. *J. Geophys. Res.,* **100,** 1367–1378.

Klein, S. A., and D. L. Hartmann, 1993: Spurious changes in the ISCCP dataset. *Geophys. Res. Lett.,* **20,** 455–458.

London, J., S. G. Warren, and C. J. Hahn, 1991: Thirty-year trend of observed greenhouse clouds over the tropical oceans. *Adv. Space Res.,* **11,** 345–349.

Mitchell, T., and J. M. Wallace, 1996: An observational study of ENSO variability in 1950–78 and 1979–92. *J. Climate,* **9,** 3149–3161.

Nicholls, N., G. V. Gruza, J. Jouzel, T. R. Karl, L. A. Ogallo, and D. E. Parker, 1996: Observed climate variability and change. *Climate Change 1995: The Science of Climate Change,* (International Panel on Climate Change, Working Group I), J. T. Houghton, L. G. Meira, B. A. Callandar, N. Harris, A. Kattenberg, and K. Marshall, Eds., Cambridge University Press, 133–192.

Nitta, T., and S. Yamada, 1989: Recent warming of tropical sea surface temperature and its relationship to the Northern Hemisphere circulation. *J. Meteor. Soc. Japan,* **67,** 375–383.

Norris, J., 1998a: Low cloud structure over the ocean from surface observations. Part I: Relationship to advection and the vertical distribution of temperature and moisture. *J. Climate,* **11,** 369–382.

——, 1998b: Low cloud structure over the ocean from surface observations. Part II: Geographical and seasonal variations. *J. Climate,* **11,** 383–403.

Oort, A. H., Y. H. Pan, R. W. Reynolds, and C. F. Ropelewski, 1987: Historical trends in the surface temperature over the oceans based on the COADS. *Climate Dyn.,* **2,** 29–38.

Quayle, R. G., 1974: A climatic comparison of ocean weather station and transient ship records. *Mar. Wea. Log,* **18,** 307–311.

Rossow, W. B., and R. A. Schiffer, 1991. International Satellite Cloud Climatology Project (ISSCP) cloud data products. *Bull. Amer Meteor. Soc.,* **72,** 2–20.

Santer, B. D., T. M. L. Wigley, T. P. Barnett, and E. Anyamba, 1995: Detection of Climate Change and Attribution of Causes. *Climate Change 1995: The Science of Climate Change,* J. T. Houghton, L. G. Meira, B. A. Callandar, N. Harris, A. Kattenberg, and K. Marshall, Eds., Cambridge University Press, 407–443.

Slingo, A., 1990: Sensitivity of the earth's radiation budget to changes in low clouds. *Quart. J. Roy. Meteor. Soc.,* **116,** 705–739.

Soden, B. J., and R. Fu, 1995: A satellite analysis of deep convection, upper-tropospheric humidity, and the greenhouse effect. *J. Climate,* **8,** 2333–2351.

Stopford, M., 1988: *Maritime Economics.* Unwin Hyman, 402 pp.

Waliser, D. E., and W. Zhou, 1997: Removing satellite equatorial crossing time biases from the OLR and HRC data sets. *J. Climate,* **10,** 2125–2146.

Warren, S. G., C. J. Hahn, J. London, R. M. Chervin, and R. L. Jenne, 1988: Global distribution of total cloud cover and cloud type amounts over the ocean. NCAR Tech. Note TN-317+STR, 170 pp. [Available from National Center for Atmospheric Research, Boulder, CO, 80307-3000.]

Wielicki, B. A., R. D. Cess, M. D. King, D. A. Randall, and E. F. Harrison, 1995: Mission to Planet Earth: Role of clouds and radiation in climate. *Bull. Amer. Meteor. Soc.,* **76,** 2125–2153.

Woodruff, S. D., R. J. Slutz, R. L. Jenne, and P. M. Seurer, 1987: A comprehensive ocean–atmosphere data set. *Bull. Amer. Meteor. Soc.,* **68,** 1239–1250.

WMO, 1956: *International Cloud Atlas, Abridged Atlas.* WMO, Vol. 1, 62 pp.

——, 1975: *Manual on the Observation of Clouds and Other Meteors.* WMO, Vol. 1, 155 pp.

Wright, P. B., 1986: Problems in the use of ship observations for the study of interdecadal climate changes. *Mon. Wea. Rev.,* **114,** 1028–1034.